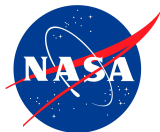


High-order cell-centered discontinuous Galerkin scheme for Lagrangian hydrodynamics

François Vilar

Brown University, Division of Applied Mathematics
182 George Street, Providence, RI 02912

May 4th, 2015



- 1 Introduction
- 2 Eulerian and Lagrangian descriptions
- 3 Two-dimensional discretization
- 4 Numerical results
- 5 Conclusion

Eulerian formalism (spatial description)

- Fixed referential attached to the observer
- Fixed observation area in which the fluid flows through

Lagrangian formalism (material description)

- Moving referential attached to the material
- Observation area getting moved and deformed through the fluid flow

Advantages of the Lagrangian formalism

- Adapted to the study of regions undergoing large shape changes
- Naturally tracks interfaces in multimaterial compressible flows
- No numerical diffusion from the discretization of the convection terms

Disadvantages of the Lagrangian formalism

- **Robustness issue in cases of shear flows or vortexes**
⇒ ALE (Arbitrary Lagrangian-Eulerian) method

- 1 Introduction
- 2 Eulerian and Lagrangian descriptions**
- 3 Two-dimensional discretization
- 4 Numerical results
- 5 Conclusion

Definitions

- ρ is the fluid density
- $\mathbf{u} = (u_1, u_2, u_3)^t$ is the fluid velocity
- e is the fluid specific total energy
- p is the fluid pressure
- $\varepsilon = e - \frac{1}{2}\mathbf{u}^2$ is the fluid specific internal energy

Euler equations

- $\frac{\partial \rho}{\partial t} + \nabla_x \cdot (\rho \mathbf{u}) = 0$ Continuity equation
- $\frac{\partial \rho \mathbf{u}}{\partial t} + \nabla_x \cdot (\rho \mathbf{u} \otimes \mathbf{u} + p \mathbf{I}_d) = \mathbf{0}$ Momentum conservation equation
- $\frac{\partial \rho e}{\partial t} + \nabla_x \cdot (\rho \mathbf{u} e + p \mathbf{u}) = 0$ Total energy conservation equation

Thermodynamical closure

- $p = p(\rho, \varepsilon)$ Equation of state (EOS)

Momentum equation

- $\frac{\partial \rho \mathbf{u}}{\partial t} + \nabla_x \cdot (\rho \mathbf{u} \otimes \mathbf{u} + p \mathbb{1}_d) = \mathbf{0}$
- $\rho \left(\frac{\partial \mathbf{u}}{\partial t} + (\nabla_x \mathbf{u}) \mathbf{u} \right) + \underbrace{\mathbf{u} \left(\frac{\partial \rho}{\partial t} + \nabla_x \cdot (\rho \mathbf{u}) \right)}_{=0} + \nabla_x p = \mathbf{0}$
- $\rho \left(\frac{\partial u_i}{\partial t} + \mathbf{u} \cdot \nabla_x u_i \right) + \nabla_x \cdot (\rho \mathbb{1}(i)) = 0$
- $\mathbb{1}(i) = (\delta_{i1}, \delta_{i2}, \delta_{i3})^t$

Total energy equation

- $\frac{\partial \rho e}{\partial t} + \nabla_x \cdot (\rho \mathbf{u} e + p \mathbf{u}) = 0$
- $\rho \left(\frac{\partial e}{\partial t} + \mathbf{u} \cdot \nabla_x e \right) + \underbrace{e \left(\frac{\partial \rho}{\partial t} + \nabla_x \cdot (\rho \mathbf{u}) \right)}_{=0} + \nabla_x \cdot (p \mathbf{u}) = 0$
- $\rho \left(\frac{\partial e}{\partial t} + \mathbf{u} \cdot \nabla_x e \right) + \nabla_x \cdot (p \mathbf{u}) = 0$

Definitions

- $\tau = \frac{1}{\rho}$ is the specific volume
- $\mathbf{U} = (\tau, u_1, u_2, u_3, e)^t$ is the variables vector
- $\mathbf{F}(\mathbf{U}) = (-\mathbf{u}, p \mathbb{1}(1), p \mathbb{1}(2), p \mathbb{1}(3), p \mathbf{u})^t$ is the flux vector

Continuity equation

- $\frac{\partial \rho}{\partial t} + \nabla_x \cdot (\rho \mathbf{u}) = 0$
- $\frac{\partial \rho}{\partial t} + \mathbf{u} \cdot \nabla_x \rho + \rho \nabla_x \cdot \mathbf{u} = 0$
- $\rho \left(\frac{\partial \tau}{\partial t} + \mathbf{u} \cdot \nabla_x \tau \right) - \nabla_x \cdot \mathbf{u} = 0$

Gas dynamics equations

- $\rho \left(\frac{\partial \mathbf{U}}{\partial t} + \mathbf{u} \cdot \nabla_x \mathbf{U} \right) + \nabla_x \cdot \mathbf{F}(\mathbf{U}) = 0$

Flow transformation of the fluid

- The fluid flow is described mathematically by the continuous transformation, Φ , so-called mapping such as $\Phi : \mathbf{X} \longrightarrow \mathbf{x} = \Phi(\mathbf{X}, t)$

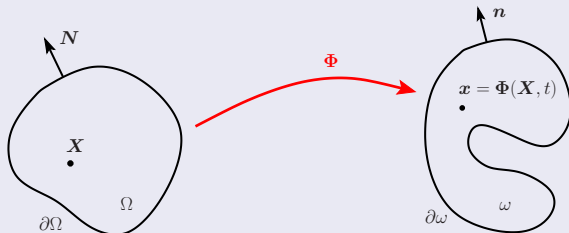


Figure : Notation for the flow map.

where \mathbf{X} is the Lagrangian (initial) coordinate, \mathbf{x} the Eulerian (actual) coordinate, \mathbf{N} the Lagrangian normal and \mathbf{n} the Eulerian normal

Flow map Jacobian matrix: deformation gradient tensor

- $\mathbf{J} = \nabla_{\mathbf{x}}\Phi = \nabla_{\mathbf{x}}\mathbf{x}$ and $|\mathbf{J}| = \det \mathbf{J} > 0$

Trajectory equation

- $\frac{\partial \mathbf{x}(\mathbf{X}, t)}{\partial t} = \mathbf{u}(\mathbf{x}(\mathbf{X}, t), t)$
- $\mathbf{x}(\mathbf{X}, 0) = \mathbf{X}$

Material time derivative

- $\varphi(\mathbf{x}, t)$ is a fluid variable with sufficient smoothness
- $\frac{d\varphi}{dt} \equiv \frac{\partial \varphi(\mathbf{x}(\mathbf{X}, t), t)}{\partial t} = \frac{\partial \varphi}{\partial t} + \mathbf{u} \cdot \nabla_{\mathbf{x}} \varphi$

Updated Lagrangian formulation

- $\rho \frac{d\mathbf{U}}{dt} + \nabla_{\mathbf{x}} \cdot \mathbf{F}(\mathbf{U}) = 0$ Moving configuration

Integral conservative form

- $\frac{\partial}{\partial t} \int_{\omega} \rho \mathbf{U} dV + \int_{\partial \omega} \mathbf{F}(\mathbf{U}) \cdot \mathbf{n} ds = 0$ Moving configuration

Transformation formulas

- $\mathbf{J} d\mathbf{X} = d\mathbf{x}$ Change of shape of infinitesimal vectors
- $|\mathbf{J}| dV = dv$ Measure of the volume change
- $|\mathbf{J}| \mathbf{J}^{-t} \mathbf{N} dS \equiv \mathbf{J}^* \mathbf{N} dS = \mathbf{n} ds$ **Nanson formula**

Mass conservation

- $\rho^0(\mathbf{X})$ is the initial fluid density
- $\int_{\Omega} \rho^0 dV = \int_{\omega} \rho dv$
- $\int_{\omega} \rho dv = \int_{\Omega} \rho |\mathbf{J}| dV$
- $\rho |\mathbf{J}| = \rho^0$

Mass integral relation

- $\frac{\partial}{\partial t} \int_{\omega} \rho \varphi dv = \frac{\partial}{\partial t} \int_{\Omega} \rho |\mathbf{J}| \varphi dV = \int_{\Omega} \rho |\mathbf{J}| \frac{\partial \varphi}{\partial t} dV$
- $\frac{\partial}{\partial t} \int_{\omega} \rho \varphi dv = \int_{\omega} \rho \frac{d\varphi}{dt} dv$

Differential operators transformations

- $\phi(\mathbf{x}, t)$ is a fluid vector valued variable with sufficient smoothness
- $\nabla_{\mathbf{x}} \cdot \phi = \frac{1}{|J|} \nabla_{\mathbf{X}} \cdot (\mathbf{J}^{*t} \phi)$

Piola compatibility condition

$$\bullet \nabla_{\mathbf{X}} \cdot \mathbf{J}^* = \mathbf{0} \implies \int_{\Omega} \nabla_{\mathbf{X}} \cdot \mathbf{J}^* dV = \int_{\partial\Omega} \mathbf{J}^* \mathbf{N} dS = \int_{\partial\omega} \mathbf{n} ds = \mathbf{0}$$

Total Lagrangian formulation

- $\frac{\partial \mathbf{J}}{\partial t} - \nabla_{\mathbf{X}} \mathbf{u} = 0$ Deformation gradient tensor
- $\rho^0 \frac{\partial \mathbf{U}}{\partial t} + \nabla_{\mathbf{X}} \cdot (\mathbf{J}^{*t} \mathbf{F}(\mathbf{U})) = 0$ Fixed configuration

Integral conservative form

- $\frac{\partial}{\partial t} \int_{\Omega} \rho^0 \mathbf{U} dV + \int_{\partial\Omega} \mathbf{F}(\mathbf{U}) \cdot \mathbf{J}^* \mathbf{N} dS = 0$ Fixed configuration

- 1 Introduction
- 2 Eulerian and Lagrangian descriptions
- 3 Two-dimensional discretization**
- 4 Numerical results
- 5 Conclusion

$(s + 1)^{\text{th}}$ order DG discretization

- $\{\Omega_c\}_c$ a partition of the domain Ω into polygonal cells
- $\{\sigma_k^c\}_{k=0\dots K}$ basis of $\mathbb{P}^s(\Omega_c)$, where $K + 1 = \frac{(s+1)(s+2)}{2}$
- $\phi_h^c(\mathbf{X}, t) = \sum_{k=0}^K \phi_k^c(t) \sigma_k^c(\mathbf{X})$ approximate function of $\phi(\mathbf{X}, t)$ on Ω_c

Definitions

- m_c constant mass of cell Ω_c
- $\mathbf{x}_c = (\mathcal{X}_c, \mathcal{Y}_c)^t = \frac{1}{m_c} \int_{\Omega_c} \rho^0(\mathbf{X}) \mathbf{X} dV$ center of mass of cell Ω_c
- $\langle \phi \rangle_c = \frac{1}{m_c} \int_{\Omega_c} \rho^0(\mathbf{X}) \phi(\mathbf{X}) dV$ mean value of function ϕ over Ω_c
- $(\phi \cdot \psi)_c = \int_{\Omega_c} \rho^0(\mathbf{X}) \phi(\mathbf{X}) \psi(\mathbf{X}) dV$ associated scalar product

Taylor expansion on the cell, located at the center of mass

$$\phi(\mathbf{X}) = \phi(\mathbf{x}_c) + \sum_{k=1}^s \sum_{j=0}^k \frac{(X - x_c)^{k-j} (Y - y_c)^j}{j!(k-j)!} \frac{\partial^k \phi}{\partial X^{k-j} \partial Y^j}(\mathbf{x}_c) + o(\|\mathbf{X} - \mathbf{x}_c\|^s)$$

$(s + 1)^{\text{th}}$ order scheme polynomial Taylor basis

- The first-order polynomial component and the associated basis function

$$\phi_0^c = \langle \phi \rangle_c \quad \text{and} \quad \sigma_0^c = 1$$

- The k^{th} -order polynomial components and the associated basis functions

$$\phi_{\frac{k(k+1)}{2}+j}^c = (\Delta X_c)^{k-j} (\Delta Y_c)^j \frac{\partial^k \phi}{\partial X^{k-j} \partial Y^j}(\mathbf{x}_c),$$

$$\sigma_{\frac{k(k+1)}{2}+j}^c = \frac{1}{j!(k-j)!} \left[\left(\frac{X - x_c}{\Delta X_c} \right)^{k-j} \left(\frac{Y - y_c}{\Delta Y_c} \right)^j - \left\langle \left(\frac{X - x_c}{\Delta X_c} \right)^{k-j} \left(\frac{Y - y_c}{\Delta Y_c} \right)^j \right\rangle_c \right],$$

where $0 < k \leq s$, $j = 0 \dots k$, $\Delta X_c = \frac{X_{\max} - X_{\min}}{2}$ and $\Delta Y_c = \frac{Y_{\max} - Y_{\min}}{2}$



H. LUO, J. D. BAUM AND R. LÖHNER, *A DG method based on a Taylor basis for the compressible flows on arbitrary grids*. J. Comp. Phys., 2008.

Outcome

- First moment associated to the basis function $\sigma_0^c = 1$ is the mass averaged value

$$\phi_0^c = \langle \phi \rangle_c$$

- The successive moments can be identified as the successive derivatives of the function expressed at the center of mass of the cell

$$\phi_{\frac{k(k+1)}{2}+j}^c = (\Delta X_c)^{k-j} (\Delta Y_c)^j \frac{\partial^k \phi}{\partial X^{k-j} \partial Y^j}(\mathbf{x}_c)$$

- The first basis function is orthogonal to the other ones

$$(\sigma_0^c \cdot \sigma_k^c)_c = m_c \delta_{0k}$$

- **Same basis functions regardless the shape of the cells** (squares, triangles, generic polygonal cells)

Total Lagrangian gas dynamics system

- $\rho^0 \frac{\partial \mathbf{U}}{\partial t} + \nabla_x \cdot (\mathbf{J}^* \mathbf{F}(\mathbf{U})) = 0$

Local variational formulations

- $$\int_{\Omega_c} \rho^0 \frac{\partial \mathbf{U}_h^c}{\partial t} \sigma_j^c dV = \sum_{k=0}^K \frac{\partial \mathbf{U}_k^c}{\partial t} \int_{\Omega_c} \rho^0 \sigma_j^c \sigma_k^c dV$$

$$= \int_{\Omega_c} \mathbf{F}(\mathbf{U}_h^c) \cdot \mathbf{J}^* \nabla_x \sigma_j^c dV - \int_{\partial \Omega_c} \overline{\mathbf{F}(\mathbf{U})} \cdot \sigma_j^c \mathbf{J}^* \mathbf{N} dS$$

- $\overline{\mathbf{F}(\mathbf{U})} = (-\bar{\mathbf{u}}, \mathbb{1}(1)\bar{p}, \mathbb{1}(2)\bar{p}, \bar{p}\bar{\mathbf{u}})^t$ is the numerical flux

Geometric Conservation Law (GCL)

- $\frac{\partial |\omega_c|}{\partial t} \equiv \frac{\partial}{\partial t} \int_{\omega_c} dV = \frac{\partial}{\partial t} \int_{\Omega_c} |\mathbf{J}| dV = \int_{\Omega_c} \rho^0 \frac{\partial \tau_h^c}{\partial t} dV$

- $\int_{\Omega_c} \rho^0 \frac{\partial \tau_h^c}{\partial t} dV = \int_{\partial \Omega_c} \bar{\mathbf{u}} \cdot \mathbf{J}^* \mathbf{N} dS$

Mass matrix properties

- $\int_{\Omega_c} \rho^0 \sigma_j^c \sigma_k^c dV = (\sigma_j^c \cdot \sigma_k^c)_c$ generic coefficient of the symmetric positive definite mass matrix
- $(\sigma_0^c \cdot \sigma_k^c)_c = m_c \delta_{0k}$ mass averaged equation is independent of the other polynomial basis components equations

Interior terms

- $\int_{\Omega_c} F(U_h^c) \cdot J^* \nabla_x \sigma_j^c dV$ is evaluated through the use of a two-dimensional high-order quadrature rule

Boundary terms

- $\int_{\partial\Omega_c} \overline{F(U)} \cdot \sigma_j^c J^* \mathbf{N} dS$ required a specific treatment to ensure the GCL
- It remains to determine the numerical fluxes

Requirements

- **Consistency** of vector $\mathbf{J}^* \mathbf{N} dS = \mathbf{n} ds$ at the interfaces of the cells
- **Continuity** of vector $\mathbf{J}^* \mathbf{N}$ at cell interfaces on both sides of the interface
- **Preservation of uniform flows**, $\mathbf{J}^* = |\mathbf{J}| \mathbf{J}^{-t}$ the cofactor matrix

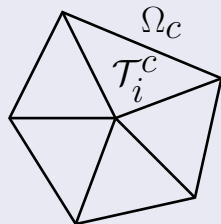
$$\int_{\Omega_c} \mathbf{J}^* \nabla_x \sigma_j^c dV = \int_{\partial\Omega_c} \sigma_j^c \mathbf{J}^* \mathbf{N} dS \iff \int_{\Omega_c} \sigma_j^c (\nabla_x \cdot \mathbf{J}^*) dV = 0$$

Generalization of the weak form of the Piola compatibility condition

Tensor J discretization

- Discretization of tensor \mathbf{J} by means of a mapping defined on triangular cells
- Partition of the polygonal cells in the initial configuration into non-overlapping triangles

$$\Omega_c = \bigcup_{i=1}^{ntri} \mathcal{T}_i^c$$



$(s + 1)^{\text{th}}$ order continuous mapping function

- We develop Φ on the Finite Elements basis functions Λ_q^i in \mathcal{T}_i of degree s

$$\Phi_h^i(\mathbf{X}, t) = \sum_{q \in \mathcal{Q}(i)} \Lambda_q^i(\mathbf{X}) \Phi_q(t),$$

where $\mathcal{Q}(i)$ is the \mathcal{T}_i control points set, including the vertices $\{p^-, p, p^+\}$

- $\Phi_q(t) = \Phi(\mathbf{X}_q, t) = \mathbf{x}_q$
- $\frac{\partial \Phi_q}{\partial t} = \bar{\mathbf{u}}_q \implies \frac{\partial}{\partial t} \mathbf{J}_i(\mathbf{X}, t) = \sum_{q \in \mathcal{Q}(i)} \bar{\mathbf{u}}_q(t) \otimes \nabla_{\mathbf{x}} \Lambda_q^i(\mathbf{X})$

Outcome

- Satisfaction of the Piola compatibility condition **everywhere**
- Consistency** and **continuity** of the Eulerian normal $\mathbf{J}^* \mathbf{N}$

Example of the fluid flow mapping in the fourth order case

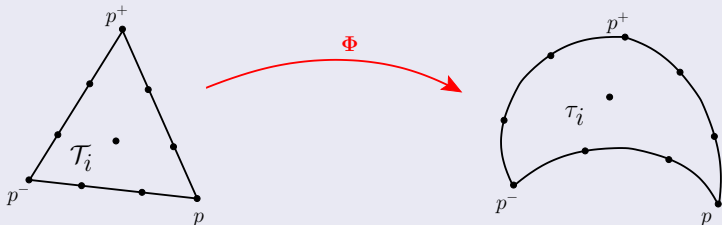


Figure : Nodes arrangement for a cubic Lagrange Finite Element mapping.

Curved edges definition using $s + 1$ control points

- Projection of the continuous mapping function Φ on the face f_{pp^+}

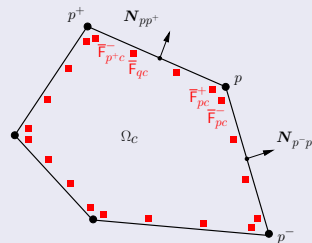
$$\mathbf{x}|_{pp^+}(\zeta) = \mathbf{x}_p \lambda_p(\zeta) + \sum_{q \in \mathcal{Q}(pp^+) \setminus \{p, p^+\}} \mathbf{x}_q \lambda_q(\zeta) + \mathbf{x}_{p^+} \lambda_{p^+}(\zeta),$$

where $\mathcal{Q}(pp^+)$ is the face control points set, $\zeta \in [0, 1]$ the curvilinear abscissa and λ_q the 1D Finite Element basis functions of degree s

Local variational formulations

$$\bullet \int_{\Omega_c} \rho^0 \frac{\partial \mathbf{U}_h^c}{\partial t} \sigma_j^c \, dV = \sum_{i=1}^{ntri} \int_{\mathcal{T}_i^c} \mathbf{F}(\mathbf{U}_h^c) \cdot \mathbf{J}^* \nabla_x \sigma_j^c \, dV$$

$$- \sum_{p \in \mathcal{P}(c)} \int_p^{p^+} \overline{\mathbf{F}}(\mathbf{U}) \cdot \sigma_j^c \mathbf{J}^* \mathbf{N} \, dL$$



Polynomial assumptions on face f_{pp^+}

$$\bullet \overline{\mathbf{F}}(\mathbf{U})|_{pp^+}(\zeta) = \overline{\mathbf{F}}_{pc}^+ \lambda_p(\zeta) + \sum_{q \in \{p, p^+\}} \overline{\mathbf{F}}_{qc} \lambda_q(\zeta) + \overline{\mathbf{F}}_{p+c}^- \lambda_{p^+}(\zeta)$$

Polynomial properties on face f_{pp^+}

$$\bullet \mathbf{J}^* \mathbf{N} \, dL|_{pp^+}(\zeta) = \mathbf{n} \, dl|_{pp^+} = \frac{\partial \mathbf{x}}{\partial \zeta} \, d\zeta|_{pp^+} \times \mathbf{e}_z = \sum_q \frac{\partial \lambda_q}{\partial \zeta}(\zeta) (\mathbf{x}_q \times \mathbf{e}_z)$$

$$\bullet \sigma_j^c|_{pp^+}(\zeta) = \sigma_j^c(\mathbf{X}_p) \lambda_p(\zeta) + \sum_{q \in \{p, p^+\}} \sigma_j^c(\mathbf{X}_q) \lambda_q(\zeta) + \sigma_j^c(\mathbf{X}_{p^+}) \lambda_{p^+}(\zeta)$$

Fundamental assumptions

- $\bar{\mathbf{u}}_{pc}^{\pm} = \bar{\mathbf{u}}_p$, $\forall c \in \mathcal{C}(p)$ and $\bar{\mathbf{u}}_{qL} = \bar{\mathbf{u}}_{qR} = \bar{\mathbf{u}}_q$

Procedure

- Analytical integration + index permutation

Weighted corner normals

- $l_{pc}^{+,j} \mathbf{n}_{pc}^{+,j} = \int_p^{p^+} \lambda_p \sigma_j \mathbf{J}^* \mathbf{N} dS$
- $l_{pc}^{-,j} \mathbf{n}_{pc}^{-,j} = \int_{p^-}^p \lambda_p \sigma_j \mathbf{J}^* \mathbf{N} dS$
- $l_{pc}^j \mathbf{n}_{pc}^j = l_{pc}^{-,j} \mathbf{n}_{pc}^{-,j} + l_{pc}^{+,j} \mathbf{n}_{pc}^{+,j}$

Weighted face control point normals

- $l_{qc}^j \mathbf{n}_{qc}^j = \int_p^{p^+} \lambda_q \sigma_j \mathbf{J}^* \mathbf{N} dS$

Semi-discrete equations GCL compatible

$$\bullet \int_{\Omega_c} \rho^0 \frac{\partial \mathbf{U}_h^c}{\partial t} \sigma_j^c dV = - \sum_{i=1}^{ntri} \int_{\mathcal{T}_i^c} \mathbf{F}(\mathbf{U}_h^c) \cdot \mathbf{J}^* \nabla_x \sigma_j^c dV$$

$$+ \sum_{\rho \in \mathcal{P}(c)} \left[\left(\bar{\mathbf{F}}_{\rho c}^- \cdot \mathbf{l}_{\rho c}^{-,j} \mathbf{n}_{\rho c}^{-,j} + \bar{\mathbf{F}}_{\rho c}^+ \cdot \mathbf{l}_{\rho c}^{+,j} \mathbf{n}_{\rho c}^{+,j} \right) + \sum_{q \setminus \{\rho, \rho^+\}} \bar{\mathbf{F}}_{qc} \cdot \mathbf{l}_{qc}^j \mathbf{n}_{qc}^j \right]$$

Entropic semi-discrete production

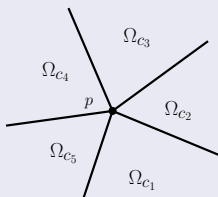
- $T dS \equiv d\varepsilon + p d\tau = d\mathbf{e} - \mathbf{u} \cdot d\mathbf{u} + p d\tau$ Gibbs identity
- Combining the different variational formulations leads to

$$\int_{\Omega_c} \rho^0 T \frac{\partial S}{\partial t} dV = \int_{\partial\Omega_c} (\bar{p} - p_h^c) (\mathbf{u}_h^c - \bar{\mathbf{u}}) \cdot \mathbf{J}^* \mathbf{N} dS$$

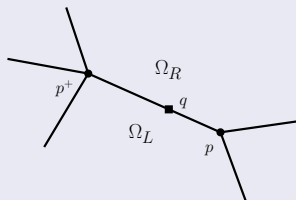
- A sufficient condition to satisfy $\int_{\Omega_c} \rho^0 T \frac{\partial S}{\partial t} dV \geq 0$ is

$$\bar{p} - p_h^c = -\tilde{z} (\bar{\mathbf{u}} - \mathbf{u}_h^c) \cdot \frac{\mathbf{J}^* \mathbf{N}}{\|\mathbf{J}^* \mathbf{N}\|} = -\tilde{z} (\bar{\mathbf{u}} - \mathbf{u}_h^c) \cdot \mathbf{n}$$

- $\tilde{z} \geq 0$ is a local approximation of the acoustic impedance $z = \rho a$



Node cell set



Face point cell set

Conservation + no boundary condition

$$\bullet \sum_c \int_{\Omega_c} \rho^0 \frac{\partial U_h^c}{\partial t} dV = 0$$

Sufficient conditions

$$\bullet \sum_{c \in \mathcal{C}(p)} \left(\bar{\rho}_{pc}^- I_{pc}^-,{}^0 \mathbf{n}_{pc}^-,{}^0 + \bar{\rho}_{pc}^+ I_{pc}^+,{}^0 \mathbf{n}_{pc}^+,{}^0 \right) = \mathbf{0}$$

Node condition

$$\bullet \bar{\rho}_{qL} I_{qL}^0 \mathbf{n}_{qL}^0 + \bar{\rho}_{qR} I_{qR}^0 \mathbf{n}_{qR}^0 = \mathbf{0}$$

Face condition

Nodal velocity

- $$\sum_{c \in \mathcal{C}(p)} [p_h^c(\mathbf{X}_p) l_{pc}^0 \mathbf{n}_{pc}^0 - M_{pc}(\bar{\mathbf{u}}_p - \mathbf{u}_h^c(\mathbf{X}_p))] = \mathbf{0}$$
- $$M_{pc} = \tilde{z}_{pc}^- l_{pc}^{-,0} (\mathbf{n}_{pc}^{-,0} \otimes \mathbf{n}_{pc}^{-,0}) + \tilde{z}_{pc}^+ l_{pc}^{+,0} (\mathbf{n}_{pc}^{+,0} \otimes \mathbf{n}_{pc}^{+,0})$$
- $$\left(\sum_{c \in \mathcal{C}(p)} M_{pc} \right) \bar{\mathbf{u}}_p = \sum_{c \in \mathcal{C}(p)} [M_{pc} \mathbf{u}_h^c(\mathbf{X}_p) + p_h^c(\mathbf{X}_p) l_{pc}^0 \mathbf{n}_{pc}^0]$$

Face control point velocity

- $$(p_h^L(\mathbf{X}_p) - p_h^R(\mathbf{X}_q)) l_{qL}^0 \mathbf{n}_{qL}^0 - M_{qL}(\bar{\mathbf{u}}_q - \mathbf{u}_h^L(\mathbf{X}_q)) - M_{qR}(\bar{\mathbf{u}}_q - \mathbf{u}_h^R(\mathbf{X}_q)) = \mathbf{0}$$
- $$M_{qc} = \tilde{z}_{qc} M_q = \tilde{z}_{qc} (l_{qL}^0 \mathbf{n}_{qL}^0 \otimes \mathbf{n}_{qL}^0)$$
- $$M_q \bar{\mathbf{u}}_q = M_q \left(\frac{\tilde{z}_{qL} \mathbf{u}_h^L(\mathbf{X}_q) + \tilde{z}_{qR} \mathbf{u}_h^R(\mathbf{X}_q)}{\tilde{z}_{qL} + \tilde{z}_{qR}} \right) - \frac{p_h^R(\mathbf{X}_q) - p_h^L(\mathbf{X}_q)}{\tilde{z}_{qL} + \tilde{z}_{qR}} l_{qL}^0 \mathbf{n}_{qL}^0$$
- $$(\bar{\mathbf{u}}_q \cdot \mathbf{n}_{qL}^0) = \left(\frac{\tilde{z}_{qL} \mathbf{u}_h^L(\mathbf{X}_q) + \tilde{z}_{qR} \mathbf{u}_h^R(\mathbf{X}_q)}{\tilde{z}_{qL} + \tilde{z}_{qR}} \right) \cdot \mathbf{n}_{qL}^0 - \frac{p_h^R(\mathbf{X}_q) - p_h^L(\mathbf{X}_q)}{\tilde{z}_{qL} + \tilde{z}_{qR}}$$

Tangential component of the face control point velocity

$$\bullet (\bar{\mathbf{u}}_q \cdot \mathbf{t}_{qL}^0) = \left(\frac{\tilde{z}_{qL} \mathbf{u}_h^L(\mathbf{X}_q) + \tilde{z}_{qR} \mathbf{u}_h^R(\mathbf{X}_q)}{\tilde{z}_{qL} + \tilde{z}_{qR}} \right) \cdot \mathbf{t}_{qL}^0$$

Face control point velocity

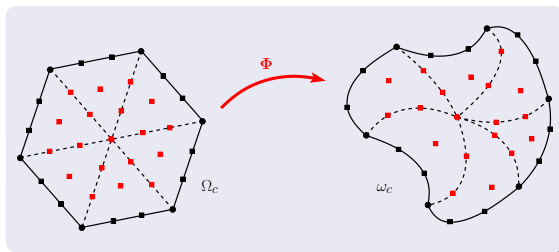
$$\bullet \bar{\mathbf{u}}_q = \left(\frac{\tilde{z}_{qL} \mathbf{u}_h^L(\mathbf{X}_q) + \tilde{z}_{qR} \mathbf{u}_h^R(\mathbf{X}_q)}{\tilde{z}_{qL} + \tilde{z}_{qR}} \right) - \frac{p_h^R(\mathbf{X}_q) - p_h^L(\mathbf{X}_q)}{\tilde{z}_{qL} + \tilde{z}_{qR}} \mathbf{n}_{qL}^0$$

Deformation tensor

$$\bullet \frac{\partial}{\partial t} \mathbf{J}_i = \sum_{Q \in \mathcal{Q}(i)} \bar{\mathbf{u}}_Q \otimes \nabla_x \Lambda_i^Q$$

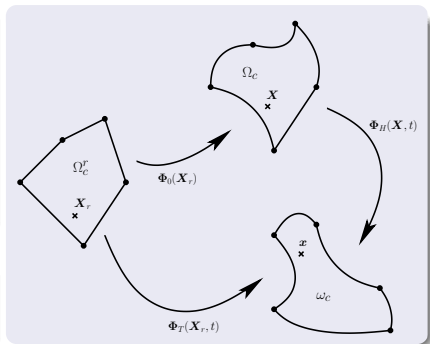
Interior points velocity

$$\bullet \bar{\mathbf{u}}_Q = \mathbf{u}_h^c(\mathbf{X}_Q, t)$$



Composed derivatives

- $$\begin{aligned} \mathbf{J}_T(\mathbf{X}_r, t) &= \nabla_{\mathbf{X}_r} \Phi_T(\mathbf{X}_r, t) \\ &= \nabla_{\mathbf{X}} \Phi_H(\mathbf{X}, t) \circ \nabla_{\mathbf{X}_r} \Phi_0(\mathbf{X}_r) \\ &= \mathbf{J}_H(\mathbf{X}, t) \mathbf{J}_0(\mathbf{X}_r) \end{aligned}$$
- $$|\mathbf{J}_T(\mathbf{X}_r, t)| = |\mathbf{J}_H(\mathbf{X}, t)| |\mathbf{J}_0(\mathbf{X}_r)|$$



Mass conservation

- $$\rho^0 |\mathbf{J}_0| = \rho |\mathbf{J}_T|$$

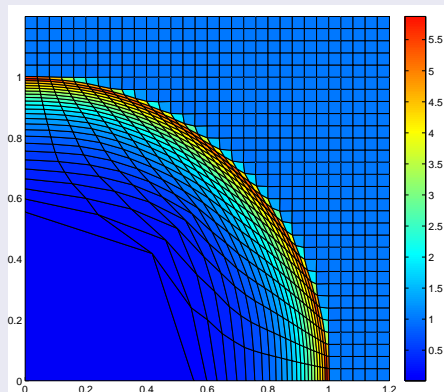
Modification of the mass matrix

- $$\int_{\omega_c} \rho \frac{\partial \psi_h^c}{\partial t} \sigma_j d\omega = \sum_{k=0}^K \frac{\partial \psi_k}{\partial t} \int_{\Omega_c^r} \rho^0 |\mathbf{J}_0| \sigma_j \sigma_k d\Omega^r$$

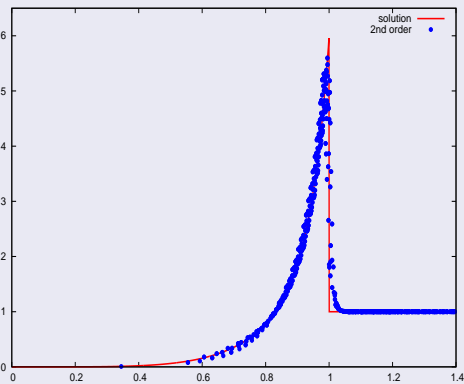
time rate of change of successive moments of function ψ
- New definitions of mass matrix, of mass averaged value and of the associated scalar product

- 1 Introduction
 - Eulerian and Lagrangian descriptions
- 2 Eulerian and Lagrangian descriptions
 - Eulerian description
 - Lagrangian descriptions
- 3 Two-dimensional discretization
 - DG general framework
 - Deformation gradient tensor
 - Discretization
 - Control point solvers
 - Initial deformation
- 4 Numerical results
 - **Second-order scheme**
 - Third-order scheme
- 5 Conclusion

Sedov point blast problem on a Cartesian grid



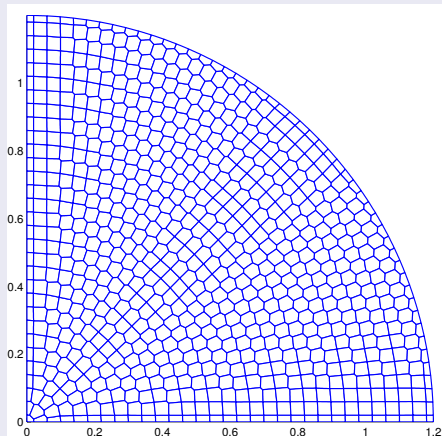
(a) Second-order scheme.



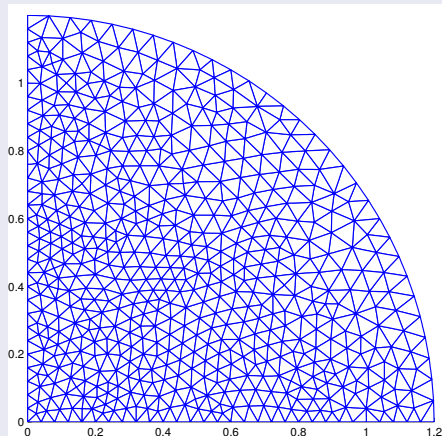
(b) Density profiles.

Figure : Point blast Sedov problem on a Cartesian grid made of 30×30 cells: density.

Sedov point blast problem on unstructured grids



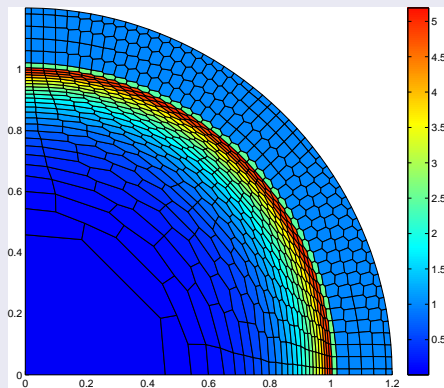
(a) Polygonal grid.



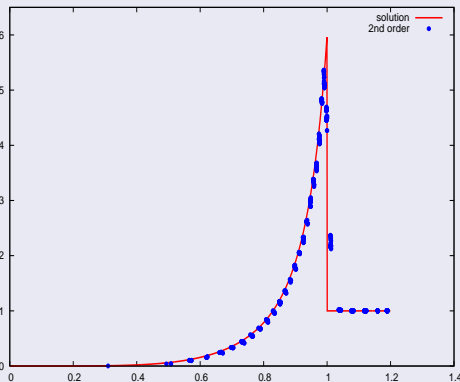
(b) Triangular grid.

Figure : Unstructured initial grids for the point blast Sedov problem.

Sedov point blast problem a polygonal grid



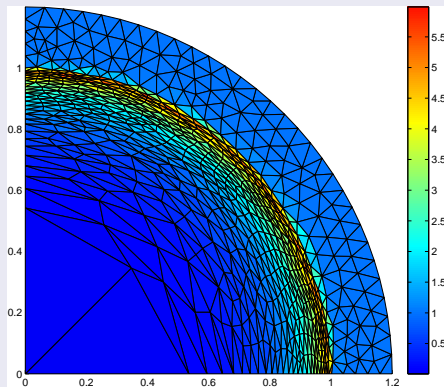
(a) Second-order scheme.



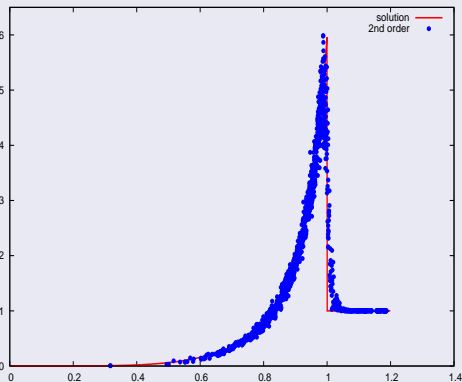
(b) Density profiles.

Figure : Point blast Sedov problem on an unstructured grid made of 775 polygonal cells: density map.

Sedov point blast problem on a triangular grid



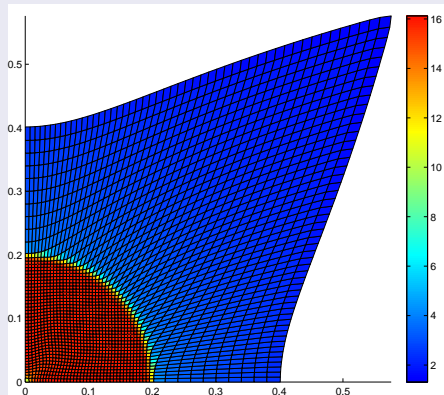
(a) Second-order scheme.



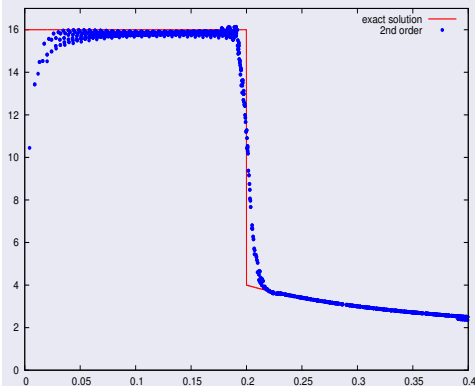
(b) Density profiles.

Figure : Point blast Sedov problem on an unstructured grid made of 1100 triangular cells: density map.

Noh problem



(a) Second-order scheme.



(b) Density profiles.

Figure : Noh problem on a Cartesian grid made of 50×50 cells: density.

Taylor-Green vortex problem

(a) Second-order scheme.

(b) Exact solution.

Figure : Motion of a 10×10 Cartesian mesh through a T.-G. vortex, at $t = 0.75$.

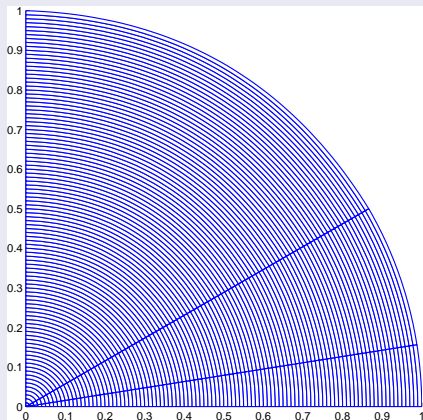
Taylor-Green vortex problem

	L_1		L_2		L_∞	
h	$E_{L_1}^h$	$q_{L_1}^h$	$E_{L_2}^h$	$q_{L_2}^h$	$E_{L_\infty}^h$	$q_{L_\infty}^h$
$\frac{1}{10}$	5.06E-3	1.94	6.16E-3	1.93	2.20E-2	1.84
$\frac{1}{20}$	1.32E-3	1.98	1.62E-3	1.97	5.91E-3	1.95
$\frac{1}{40}$	3.33E-4	1.99	4.12E-4	1.99	1.53E-3	1.98
$\frac{1}{80}$	8.35E-5	2.00	1.04E-4	2.00	3.86E-4	1.99
$\frac{1}{160}$	2.09E-5	-	2.60E-5	-	9.69E-5	-

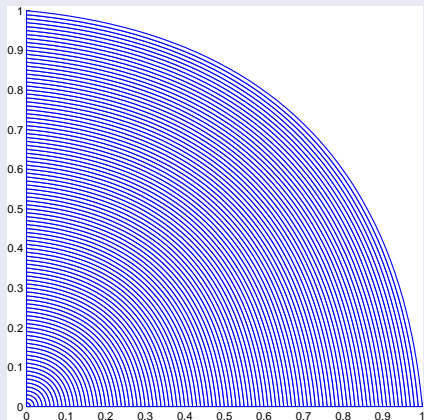
Table : Rate of convergence computed on the pressure at time $t = 0.1$.

- 1 Introduction
 - Eulerian and Lagrangian descriptions
- 2 Eulerian and Lagrangian descriptions
 - Eulerian description
 - Lagrangian descriptions
- 3 Two-dimensional discretization
 - DG general framework
 - Deformation gradient tensor
 - Discretization
 - Control point solvers
 - Initial deformation
- 4 Numerical results
 - Second-order scheme
 - **Third-order scheme**
- 5 Conclusion

Polar grids



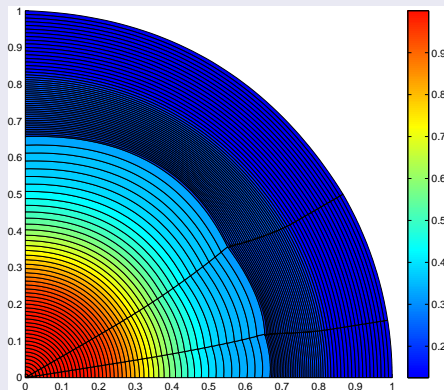
(a) Non-uniform grid.



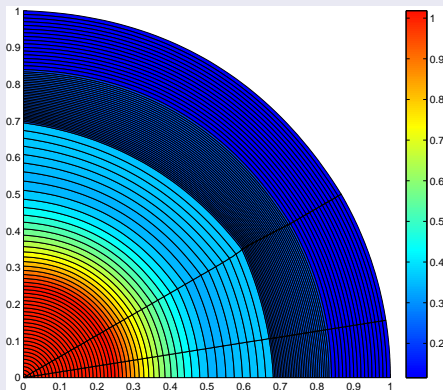
(b) One angular cell grid.

Figure : Polar initial grids for the Sod shock tube problem.

Symmetry preservation



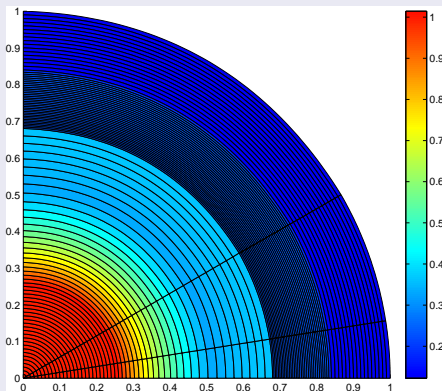
(a) First-order scheme.



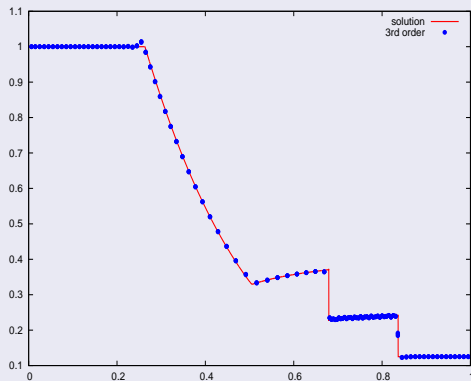
(b) Second-order scheme.

Figure : Sod shock tube problem on a polar grid made of 100×3 non-uniform cells.

Symmetry preservation



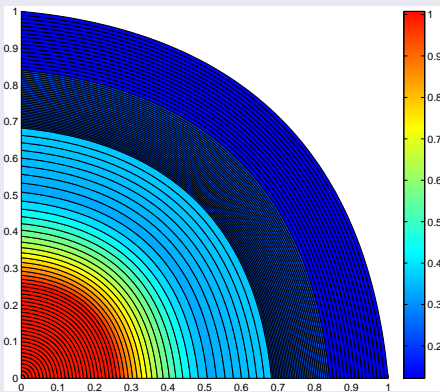
(a) Density map.



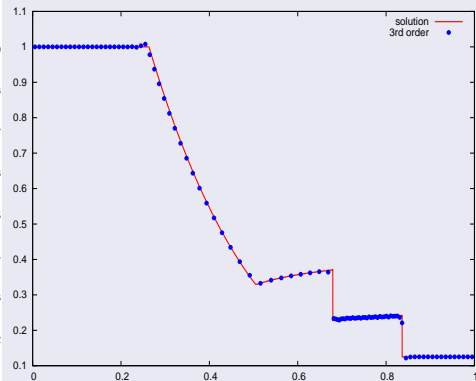
(b) Density profiles.

Figure : Third-order DG solution for a Sod shock tube problem on a polar grid made of 100×3 non-uniform cells.

One angular cell polar Sod shock tube problem



(a) Density map.



(b) Density profiles.

Figure : Third-order DG solution for a Sod shock tube problem on a polar grid made of 100×1 cells.

Variant of the incompressible Gresho vortex problem

(a) First-order scheme.

(b) Second-order scheme.

Figure : Motion of a polar grid defined in polar coordinates by $(r, \theta) \in [0, 1] \times [0, 2\pi]$, with 40×18 cells at $t = 1$: zoom on the zone $(r, \theta) \in [0, 0.5] \times [0, 2\pi]$.

Variant of the incompressible Gresho vortex problem

(a) Third-order scheme.

(b) Exact solution.

Figure : Motion of a polar grid defined in polar coordinates by $(r, \theta) \in [0, 1] \times [0, 2\pi]$, with 40×18 cells at $t = 1$: zoom on the zone $(r, \theta) \in [0, 0.5] \times [0, 2\pi]$.

Variant of the Gresho vortex problem

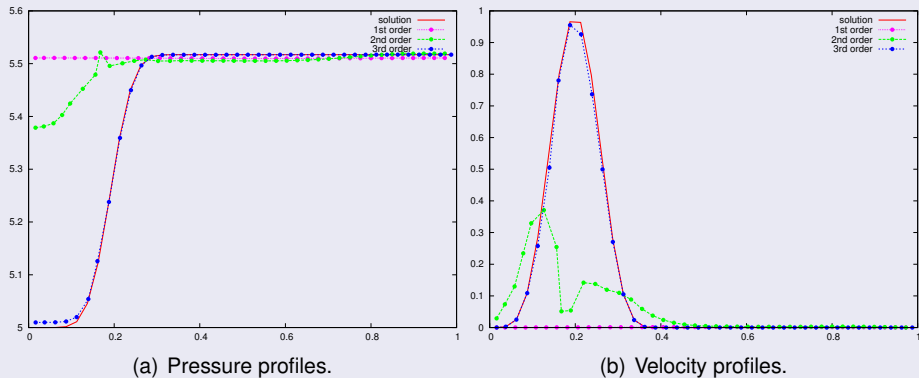


Figure : Gresho variant problem on a polar grid defined in polar coordinates by $(r, \theta) \in [0, 1] \times [0, 2\pi]$, with 40×18 cells at $t = 1$.

Variant of the Gresho vortex problem

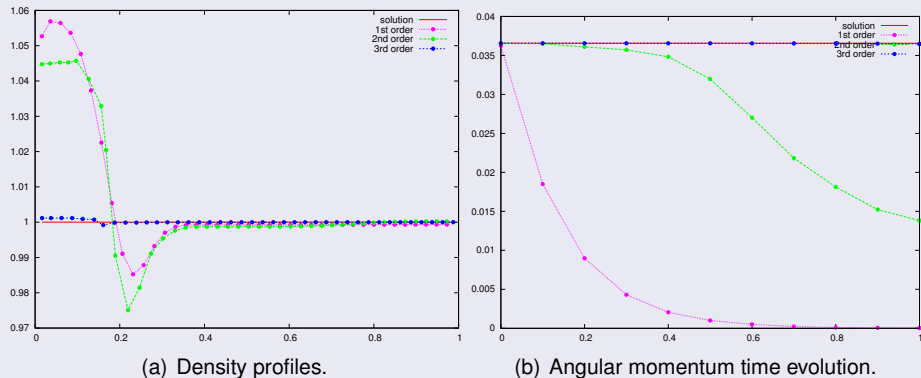
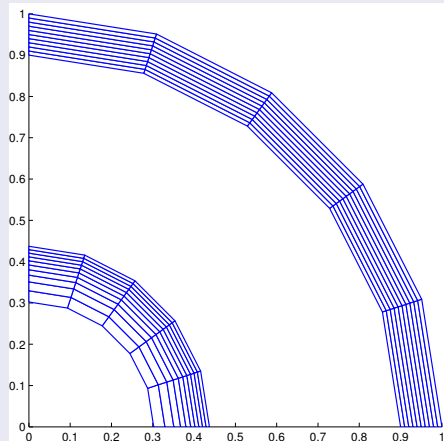
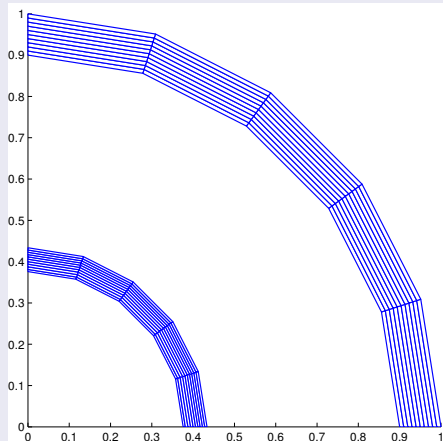


Figure : Gresho variant problem on a polar grid defined in polar coordinates by $(r, \theta) \in [0, 1] \times [0, 2\pi]$, with 40×18 cells at $t = 1$.

Kidder isentropic compression



(a) First-order solution.



(b) Second-order solution

Figure : First-order and second-order DG solutions for a Kidder isentropic compression problem on a polar grid made of 10×5 cells.

Kidder isentropic compression

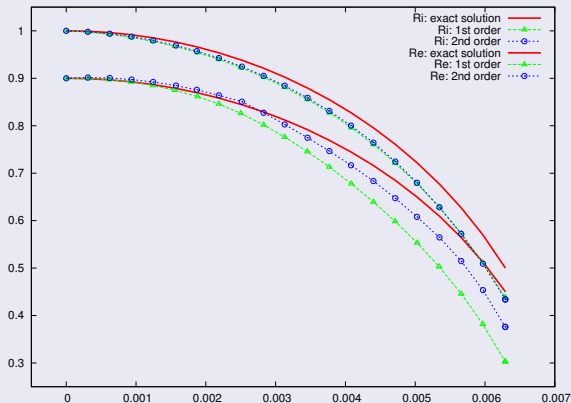
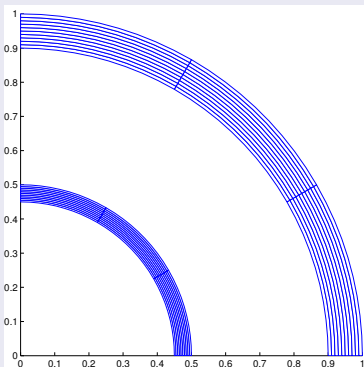
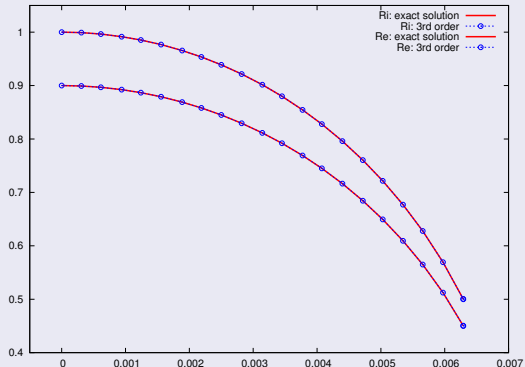


Figure : First-order and second-order DG solutions for a Kidder isentropic compression problem on a polar grid made of 10×5 cells: shell radii evolution.

Kidder isentropic compression



(a) Meshes at time $t = 0$ and $t = t_f$.



(b) Shell radii evolution.

Figure : Third-order DG solution for a Kidder isentropic compression problem on a polar grid made of 10×3 cells.

Taylor-Green vortex problem

(a) Third-order scheme.

(b) Exact solution.

Figure : Motion of a 10×10 Cartesian mesh through a T.-G. vortex, at $t = 0.75$.

Taylor-Green vortex problem

	L_1		L_2		L_∞	
h	$E_{L_1}^h$	$q_{L_1}^h$	$E_{L_2}^h$	$q_{L_2}^h$	$E_{L_\infty}^h$	$q_{L_\infty}^h$
$\frac{1}{10}$	2.67E-4	2.96	3.36E-4	2.94	1.21E-3	2.86
$\frac{1}{20}$	3.43E-5	2.97	4.36E-5	2.96	1.66E-4	2.93
$\frac{1}{40}$	4.37E-6	2.99	5.59E-6	2.98	2.18E-5	2.96
$\frac{1}{80}$	5.50E-7	2.99	7.06E-7	2.99	2.80E-6	2.99
$\frac{1}{160}$	6.91E-8	-	8.87E-8	-	3.53E-7	-

Table : Rate of convergence computed on the pressure at time $t = 0.1$.

Taylor-Green vortex problem

D.O.F	N	$E_{L_1}^h$	$E_{L_2}^h$	$E_{L_\infty}^h$	time (sec)
600	24×25	2.67E-2	3.31E-2	8.55E-2	2.01
2400	48×50	1.36E-2	1.69E-2	4.37E-2	11.0

Table : First-order DG scheme at time $t = 0.1$.

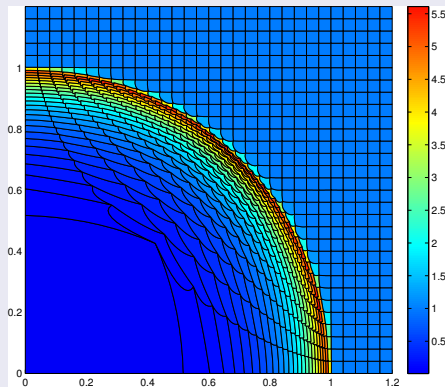
D.O.F	N	$E_{L_1}^h$	$E_{L_2}^h$	$E_{L_\infty}^h$	time (sec)
630	14×15	2.76E-3	3.33E-3	1.07E-2	2.77
2436	28×29	7.52E-4	9.02E-4	2.73E-3	11.3

Table : Second-order DG scheme without limitation at time $t = 0.1$.

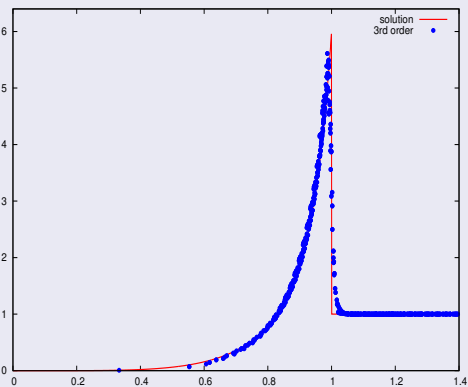
D.O.F	N	$E_{L_1}^h$	$E_{L_2}^h$	$E_{L_\infty}^h$	time (sec)
600	10×10	2.67E-4	3.36E-4	1.21E-3	4.00
2400	20×20	3.43E-5	4.36E-5	1.66E-4	30.6

Table : Third-order DG scheme without limitation at time $t = 0.1$.

Sedov point blast problem on a Cartesian grid



(a) Third-order scheme.



(b) Density profiles.

Figure : Point blast Sedov problem on a Cartesian grid made of 30×30 cells: density.

- 1 Introduction
- 2 Eulerian and Lagrangian descriptions
- 3 Two-dimensional discretization
- 4 Numerical results
- 5 Conclusion**




Conclusions

- Development of generic high-order DG schemes for the 2D gas dynamics system in a total Lagrangian formalism
- **GCL and Piola compatibility condition ensured by construction**
- **Dramatic improvement of symmetry preservation and angular momentum conservation by means of third-order DG scheme**
- Analytical proof of the positivity-preserving property of these schemes, from the first-order to the high-orders by means of a special limitation



Perspectives

- High-order limitation on moving high-order geometries
- Extension to ALE
- Extension to magnetohydrodynamics (FCM)
- Code parallelization
- Extension to 3D

Articles published on this topic

-  F. VILAR, P.-H. MAIRE and R. ABGRALL, *Cell-centered discontinuous Galerkin discretizations for two-dimensional scalar conservation laws on unstructured grids and for one-dimensional lagrangian hydrodynamics*. Computers and Fluids, 2010.
-  F. VILAR, *A discontinuous Galerkin discretization for solving the two-dimensional gas dynamics equations written under total lagrangian formulation on general unstructured grids*. Computers and Fluids, 2012.
-  F. VILAR, P.-H. MAIRE and R. ABGRALL, *A discontinuous Galerkin discretization for solving the two-dimensional gas dynamics equations written under total lagrangian formulation on general unstructured grids*. Journal of Computational Physics, 2014.

Articles in preparation on this topic

-  F. VILAR, P.-H. MAIRE and C.-W. SHU, *Positivity preservation property of cell-centered lagrangian schemes. Part I: First-order methods*.
-  F. VILAR, P.-H. MAIRE and C.-W. SHU, *Positivity preservation property of cell-centered lagrangian schemes. Part II: Extension to high-orders*.